J. Appl. Comput. Mech., 5(1) (2019) 1-12
DOI: 10.22055/JACM.2018.24099.1171

ISSN: 2383-4536
jacm.scu.ac.ir

M&MoCS
Shahid Chamran University of Ahvaz

Journal of
Applied and Computational Mechanics

Research Paper

Extension Ability of Reduced Order Model of Unsteady Incompressible Flows Using a Combination of POD and Fourier Modes

Mohammad Kazem Moayyedi

CFD, Turbulence and Combustion Research Laboratory, Department of Mechanical Engineering, University of Qom, Iran.

Received November 14 2017; Revised March 18 2018; Accepted for publication March 19 2018.
Corresponding author: M.K. Moayyedi, mk.moayyedi@qom.ac.ir

Abstract. In this article, an improved reduced order modelling approach, based on the proper orthogonal decomposition (POD) method, is presented. After projecting the governing equations of flow dynamics along the POD modes, a dynamical system was obtained. Normally, the classical reduced order models do not predict accurate time variations of flow variables due to some reasons. The response of the dynamical system was improved using a calibration method based on a least-square optimization process. The calibration polynomial can be assumed as the pressure correction term which is vanished in projecting the Navier-Stokes equations along the POD modes. The above least- square procedure is a combination of POD method and the solution of an optimization problem. The obtained model can predict accurate time variations of flow field with high speed. For long time periods, the calibration term can be computed using a combined form of POD and Fourier modes. This extension is a totally new extension to this procedure which has recently been proposed by the authors. The results obtained from the calibrated reduced order model show close agreements to the benchmark DNS data, proving high accuracy of our model.

Keywords: Proper orthogonal decomposition, Galerkin projection, Reduced order model, Calibration strategy, Incompressible flow, Fourier modes.

1. Introduction

The POD reduced order models have generated new bases in computational engineering sciences. These models, which are obtained from the conservation laws, increase the speed of computations. They have provided the adequate base for coupling different dynamical systems and have helped the researchers and engineers to test and validate their new ideas and theories. Usually, these models do not predict the accurate time variations of dynamical systems due to some reasons. The POD approximations contain two types of errors, one from the projection and the other from the modeling and the integration. The first type of error is relevant to the projection procedure, for example, the snapshots resolution. The second type of error is due to some reduced order model construction assumption. These reasons have led to more efforts to reduce these errors and accomplish accurate low order models.

Different ways for the calibration of a dynamical system have been presented to improve the prediction of POD low order models. Noack stated that the effects of pressure term cannot be eliminated in some problems because the conservation of equations is corrupted. Based on this fact, he proposed a direct substitution method of this term from the related snapshots or the solution of an adjoint equation (Noack, 2005).

The balanced POD which uses Non-linear Galerkin definition is one of the methods to improve the dynamical system prediction (Rowely, 2005). Sirisup used spectral vanishing viscosity method, which had been introduced in LES concepts, to improve the responses of POD ROM in long time periods. However, some difficulties exist and a special manner should be used in the computation procedure of dissipation term coefficients (Sirisup, 2004).

POD-α, which uses Helmholtz filtering method for Non-linear terms, has been applied for stabilization and error reduction of low dimensional dynamical systems (Sabetghadam, 2010).

Therefore, the minimization approaches are general and practical methods which have been used and defined in different forms. These methods reduce the error between the higher dimensional dynamical system and the low order model using a least-square optimization manner. Therefore, the outcome model will be stabilized. These approaches have led to a system of equations which has not a unique solution. It is because the number of known variables is less than the unknowns and therefore an important problem arises when applying these approaches (Couplet, 2005), (Favier, 2006), (Galleti, 2004) and (Moayyedi, 2009).

To improve the prediction of a dynamical system, a calibration strategy based on a least-square optimization method was used while the calibration polynomial coefficients were calculated. Two extensions of this strategy exist. One type of these methods is based on the global minimization in time and modal space. Nontheless, a new least-square-based local calibration method is introduced and used in this research to calculate free parameters in the low-dimensional POD-Galerkin systems in order to improve their short-term as well as long-term behavior (Moayyedi, 2009; Sabetghadam, 2010).

A coupled approach of SVD method and POD technique has been used to establish a reduced order finite difference extrapolation algorithm to solve non-stationary Navier-Stokes equations (Zhendong Luo, 2013).

Finite volume based reduced order model has been reconstructed for two-dimensional viscoelastic equations. The model uses fully discrete finite volume element algorithm with fewer degrees of freedom and sufficiently high accuracy based on the POD method (Hong Li, 2013).

A POD-based reduced order stabilized mixed finite volume element (SM-FVE) extrapolating model has been established with very few degrees of freedom for the non-stationary incompressible Boussinesq equations. In this model, an error estimation between the classical SMFVE solutions and the POD-based reduced-order SMFVE solutions was used for implementing the algorithm for the POD-based reduced-order SMFVE extrapolating model (Zhendong Luo, 2013).

Chen used proper orthogonal decomposition (POD) to establish reduced-order model of viscoelastic turbulent channel flow. The ROM has been based on small sets of basis functions from the POD of the sampling data obtained by direct numerical simulation (DNS) for the studied flow (Jingjing Chen, 2017).

The instability growing up in the reduced order models is due to the lack of description for the pressure term. The POD reduced order models of incompressible flows are constructed using modal coefficients of the velocity field. Therefore, it is favorable that the pressure term be represented as a function of these coefficients (Moayyedi, 2018).

The calibration method is based upon distance-minimization of the low-dimensional calibrated system and the full dynamical system in the phase space, where the independent variable is not necessarily time. To show flexibility of the method, the classical incompressible unsteady two-dimensional flow past a square cylinder at Reynolds number of 100 (vortex shedding) is addressed. For this case, the snapshots are generated by the high resolution Direct Numerical Simulation (DNS) of the Navier- Stokes equations (NSE) in the primitive variables formulation. All results are compared with DNS data and show that the calibrated dynamical system perfectly follows the real system dynamics. Using spectral functions in analyzing the behavior of dynamical systems has been initiated from a simple model such as Fourier expansion of functions to more sophisticated methods such as FEM. Fourier functions are used for the representation of each arbitrary function. In fact, if these functions have a relatively harmonic behavior, there will be a higher convergence for Fourier expansions. The calibration term in the governing equation is replaced using Fourier functions. Therefore, an autonomous dynamical system can be constructed which can predict the time evolution of the flow field.

In the sequel, the mathematical formulation of the classical POD model is presented for the Navier-Stokes equations. In the next section, Galerkin projection of NSE's and the related low-order dynamical system are discussed. The calibration of dynamical system, the least-square procedure, the long-time extension of accurate low-order model, and our results will be discussed in the following sections.

2. Representation of Navier-Stokes Equations using POD Modes

Since the POD eigenfunctions satisfy the continuity equation, the governing equations for an incompressible flow are reduced only to momentum equations which will be as follows in non-dimensional form:

$$\partial_t \mathbf{u} + (\mathbf{u}.\nabla)\mathbf{u} = -\nabla p + \frac{1}{Re}\nabla^2\mathbf{u}, \tag{1}$$

Let us rewrite the velocity vector as the summation of mean and the fluctuation parts, as:

$$\mathbf{u} = \overline{\mathbf{u}} + \mathbf{u}' \tag{2}$$

The first part is a time-averaged value of velocity component snapshots while the second part can be written using the expansion of the POD eigenfunctions as (Moayyedi 2009):

$$\mathbf{u}' = \sum_{i=1}^{N} \mathbf{a}^i(t)\Phi^i(\vec{x}) \tag{3}$$

where,

$$\mathbf{a}^i(t) = \begin{bmatrix} a^i(t) & 0 \\ 0 & b^i(t) \end{bmatrix} \quad , \quad \Phi(\vec{x}) = \begin{bmatrix} \phi_u^i(\vec{x}) \\ \phi_v^i(\vec{x}) \end{bmatrix} \tag{4}$$

In the above equations, N is number of modes, $a^i(t)$ and $\phi_u^i(\vec{x})$ are modal coefficients and the modes of streamwise velocity component, respectively. Moreover, $b^i(t)$ and $\phi_v^i(\vec{x})$ are the modal coefficients and the modes of transverse velocity component.

3. Galerkin Projection and Reduced Order POD Dynamical Model

If the incompressible Navier-Stokes equation (Eq. 1) is expanded using Eqn's. (2) and (3), based on the assumption that time derivative of the mean part is zero, new relations are obtained. These equations are projected along the POD modes and a system of ODE's is obtained which is called a dynamical system, as:

$$\frac{d\mathbf{a}^k}{dt} + \mathbf{A}_{kij}\mathbf{a}^i\mathbf{a}^j + \mathbf{B}_{ki}\mathbf{a}^i + \mathbf{C}_k = 0. \tag{5}$$

The above equation must be solved to compute the time variations of modal coefficients to be used for the reconstruction of the flow field.

3.1 Discretization of ROM Equation and Calculation of Model Coefficients

Derivatives associated with the dynamical system coefficients were computed with central finite differences of second-order accuracy. An explicit, fourth-order-accurate, four-stage Runge-Kutta scheme was used for the time integration of the ROM equations. A time step study showed that the step size (equal to DNS snapshots increment) used in this test case was adequately small. The time derivatives for minimization problem were computed using the fourth-order-accurate scheme.

3.2 Spatial discretization

For spatial discretization of each coefficient in Eq. (5), which includes spatial derivatives of velocity vector, a second order finite difference discretization method is used. The central difference formulation for interior nodes of computational domain is as follows:

$$\frac{\partial F}{\partial x} = \frac{F_{i+1,j} - F_{i-1,j}}{2\Delta x}, \tag{6}$$

For the points on the boundaries, a forward or backward second-order differential formula is used as follows:

$$\frac{\partial F}{\partial x} = \frac{-3F_{i,j} + 4F_{i+1,j} - F_{i+2,j}}{2\Delta x}, \qquad \frac{\partial F}{\partial x} = \frac{3F_{i,j} - 4F_{i-1,j} + F_{i-2,j}}{2\Delta x}. \tag{7}$$

3.3 Temporal Integration

Time discretization of the dynamical system equation is performed using the fourth-order Explicit Runge-Kutta method. This method is a convenient and accurate way for time integration of governing equations of unsteady problems.

3.4 Criterion for Choosing the Number of Modes

Normally, when the number of modes is increased, the reconstruction is performed with better accuracy. It is required to use the optimal number of modes for data reconstruction. This is equivalent to capturing the highest level of energy and the least number of modes for model construction. In this manner, a fraction number is defined for automatic selection of modes as follow:

$$\kappa = \frac{\sum_{i=1}^{N_m} \lambda_i}{\sum_{i=1}^{N_{total}} \lambda_i}, \tag{8}$$

where, κ is about 99.9% and N_m is the optimum number of modes for reduced order model construction (Moayyedi 2009).

4. Instability of the Surrogate Reduced Order Model

Classical reduced order models, which are derived from the projection of incompressible flow governing equations along the flow field modes, may not have high accuracy in predicting time variations of the field of flow. This is due to some reasons such as: (i) the absence of a direct relationship between the velocity field and the pressure [9], (ii) consequently, the approximation of the effects of neglecting the pressure term, (iii) low accuracy of the computed modes, (iv) the instability caused by truncating of high wave number modes, and (v) the low resolution input data which do not fully satisfy the conservation equations.

If the POD modes do not satisfy the continuity equation, then the effect of the mass conservation in the equation of the

ROM will be eliminated and this will cause instability in its response. The pressure term after the projection of the linear momentum conservation equation, and based on Gauss's theory, is decomposed as follows:

$$\left(\nabla p,\phi^k\right)=-\left(\nabla.\phi^k,p\right)_\Omega+\left(p,\phi^k\right)_\Gamma \tag{9}$$

If the POD modes are divergence free, they satisfy the continuity equation as:

$$\left(\nabla.\phi^k,p\right)_\Omega=0 \tag{10}$$

Then, Eq. (9) is reduced to:

$$\left(\nabla p,\phi^k\right)=\left(p,\phi^k\right)_\Gamma \tag{11}$$

The existence of homogeneous boundary conditions on all boundaries causes the elimination of the right hand side of Eq. (9). This means that the amount of pressure on the boundaries is zero or its distribution is in such a way that the inner product of the right hand side of Eq. (11) will be zero.

One of the calibration methods, which is proposed for pressure term treatment of the reduced order model, is based on direct representation of pressure using its related snapshots (Moayyedi 2018). The calibrated ROM using this approach will be:

$$\frac{d\mathbf{a}^k}{dt}+\mathbf{A}_{kij}\mathbf{a}^i\mathbf{a}^j+\left(\mathbf{B}_{ki}+\mathbf{B}_{ki}^p\right)\mathbf{a}^i+\mathbf{C}_k=0. \tag{12}$$

where $\mathbf{B}_{ki}^p$, is the related coefficient of the pressure term. Another method for calibration of low-dimensional dynamical system of N-S equation is based on the distance-minimization method. Therefore, the outcome calibrated ROM equation is as follows:

$$\frac{d\mathbf{a}^k}{dt}+\mathbf{A}_{kij}\mathbf{a}^i\mathbf{a}^j+\left(\mathbf{B}_{ki}+\mathbf{B}_{ki}'\right)\mathbf{a}^i+\mathbf{C}_k=0. \tag{13}$$

where $\mathbf{B}_{ki}'$, is the linear calibration coefficient. It can behave as a dissipation term to reduce the effect of instability sources such as high energy level modes.

4.1 Calibration of Reduced Order POD Model

In order to improve the time prediction of the reduced order POD-Galerkin model, a calibration method was used for the simple configuration of the DNS square cylinder results, which is introduced later. Using the calibration methods to improve the system increases the computational costs. However, we expect to be able to decrease the cost of the ODE's system computations by ''mixing'' the Galerkin method with a calibration method. It is achieved by calculating only a ''minimum'' number of POD-Galerkin polynomial coefficients and then evaluating the others by some optimization process. Moreover, the calibration methods optimize the coefficients of the quadratic vector polynomial associated with the reduced-order POD-Galerkin system. The problem is solved by considering the coefficients of the vector polynomials with M components of degree 2 in M variables.

4.2 Least-Square Procedure

The method proposed for the computation of the calibration terms corresponds to a simple least-mean-square procedure as follow:

$$J=\sum_{i=1}^{N_m}\left[\dot{\mathbf{a}}^i(t)-\dot{\hat{\mathbf{a}}}^i(t)+\sum_{j=1}^{N_m}B_{ij}'\times\mathbf{a}^j(t)\right]^2, \tag{14}$$

where $\dot{\hat{\mathbf{a}}}(t)$ denotes the time derivative values of modal coefficients from the DNS data using a fourth order sche me, $\dot{\mathbf{a}}(t)$ denotes the derivative of modal coefficients in time from the reduced order dynamical system, and $\mathbf{B}_{kj}'$ is the tensor of calibration coefficients. This formulation leads to a local minimization procedure for this problem in time. Since the DNS data are obtained from a high resolution field and the time increment is substantially small, the local calibration is very similar to the global one. Thus, the dynamical system with the current calibration strategy leads to relatively good results, even for long time integration presented in the next section.

4.3 Long Time Extension to Calibrated POD Model Using Fourier Series

The calibrated POD model, which was used in short time simulations, must be modified to be applicable in long time periods. In this way, the linear calibration term is modeled using Fourier sine and cosine series as:

$$\mathbf{B}_{ij}'=\frac{\tilde{a}_0}{2}+\sum_{n=1}^{N_f}\left[\tilde{a}_n\cos\left(\frac{n\pi t}{T}\right)+\tilde{b}_n\sin\left(\frac{n\pi t}{T}\right)\right]. \tag{15}$$

Obviously, the Fourier series coefficients are calculated as:

$$\tilde{a}_0 = \frac{1}{T}\int_0^T \mathbf{B}'_{ki}(t)dt\,, \qquad \tilde{a}_n = \frac{\int_0^T \mathbf{B}'_{ki}(t)\cos\left(\frac{n\pi t}{T}\right)dt}{\int_0^T \cos^2\left(\frac{n\pi t}{T}\right)dt}, \qquad \tilde{b}_n = \frac{\int_0^T B'_{ki}(t)\sin\left(\frac{n\pi t}{T}\right)dt}{\int_0^T \sin^2\left(\frac{n\pi t}{T}\right)dt}. \tag{16}$$

Therefore, the autonomous calibrated POD reduced order model is:

$$\frac{d\hat{\mathbf{a}}^k}{dt} + \mathbf{A}_{kij}\hat{\mathbf{a}}^i\hat{\mathbf{a}}^j + \left(\mathbf{B}_{ki} + \frac{\tilde{a}_o^{ki}}{2} + \sum_{n=1}^{N_f}\left[\tilde{a}_n^{ki}\cos\left(\frac{n\pi t}{T}\right) + \tilde{b}_n^{ki}\sin\left(\frac{n\pi t}{T}\right)\right]\right)\hat{\mathbf{a}}^i + \mathbf{C}_k = 0. \tag{17}$$

5. Direct Numerical Simulation of Flow Field

The CFD snapshots for the flow past a square cylinder test case were generated using a two-dimensional incompressible Navier-Stokes solver based on a finite volume method (Moayyedi 2009).

6. Results and Discussion

The results obtained for an unsteady incompressible flow past a square cylinder are demonstrated in this section. For validation of reduced order POD model, the related results were compared with the DNS data. An ensemble with 240 members in different time steps with equal time increments and in a specific time span was considered as input. Note that this time span is a complete oscillation cycle, where its length is obtained from the kinetic energy or from the non-dimensional coefficient (e.g., lift coefficient) variations versus time.

After solution of the eigenvalue problem, the POD modes were calculated. In fig. 1, contours of the four strongest modes of streamwise and transverse velocities are shown. Fig. 2 shows the energy spectrum of the first twenty POD modes for both velocity components. The symmetry and duality of the modes are seen in these figures. This is due to the similarity between POD and Fourier modes. Note that the criteria for choosing the number of modes can be verified from these graphs. Based on the criteria for the low-order model construction, seven modes were used for the construction of the reduced order model of this problem, which can capture 99.9% of the field's energy.

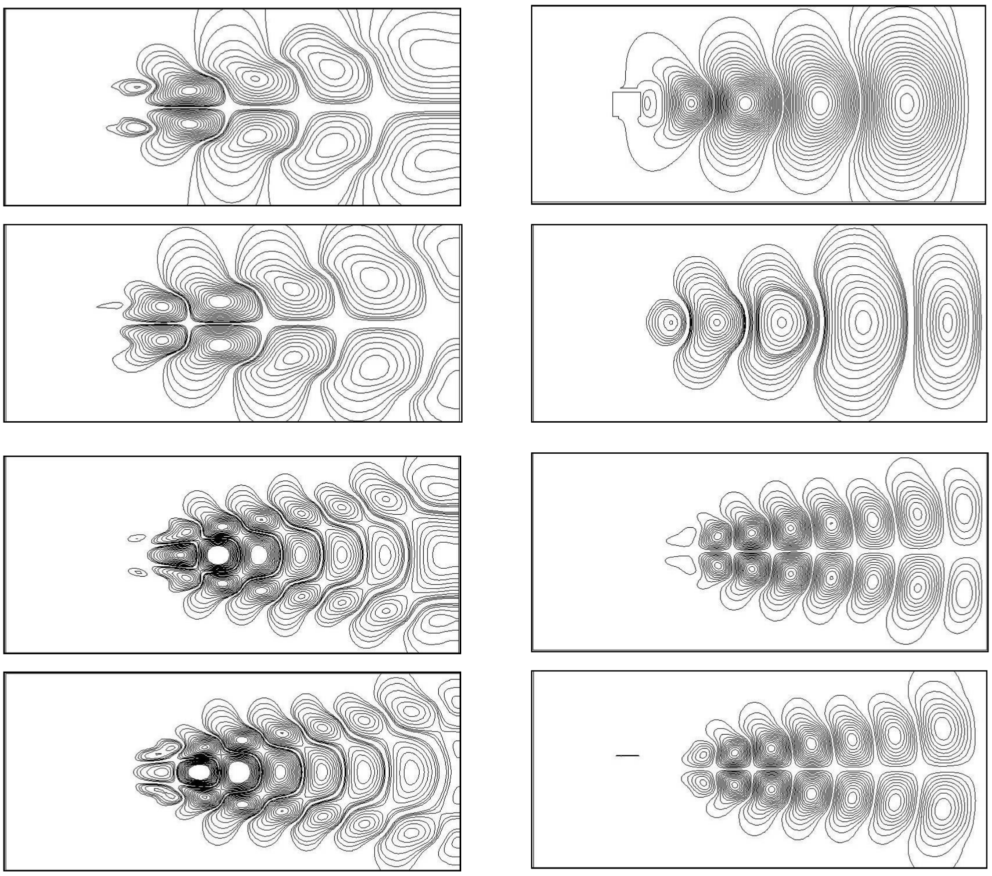

Fig. 1. Contours of the four strongest modes of streamwise velocity component (left) and transverse velocity component (right) for flow past a square cylinder at R_e=100 .

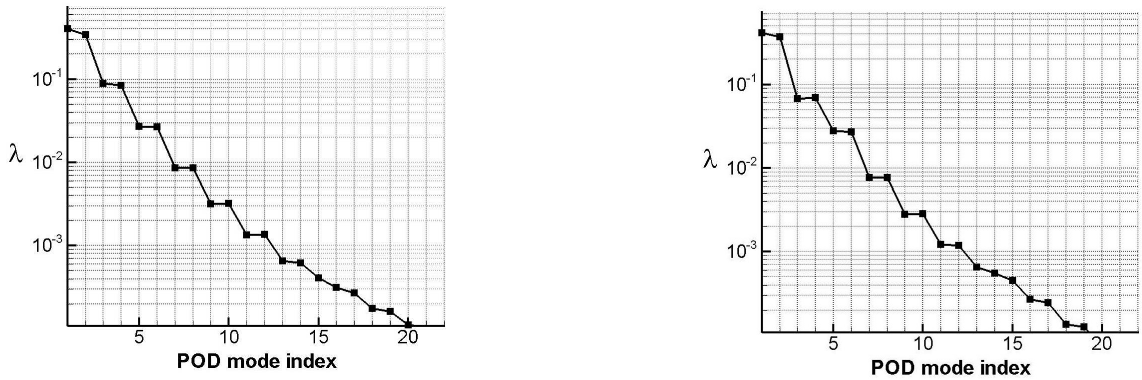

Fig. 2. Energy spectrum of POD modes in logarithmic scale, streamwise (left) and transverse (right) velocity components at $R_e = 100$.

6.1 Short Time Period Simulation

Using the method presented in the previous section, the low-order model was reconstructed using seven modes. After constructing the model, the time marching was performed using an initial condition equal to the modal coefficients (obtained from the snapshots projection) in the first time step. In Fig. 3, the time variations of the first four modal coefficients of streamwise velocity component for classical and calibrated reduced order model (compared to DNS data) are shown. It is obvious from this figure that the calibrated model predicts relatively accurate results.

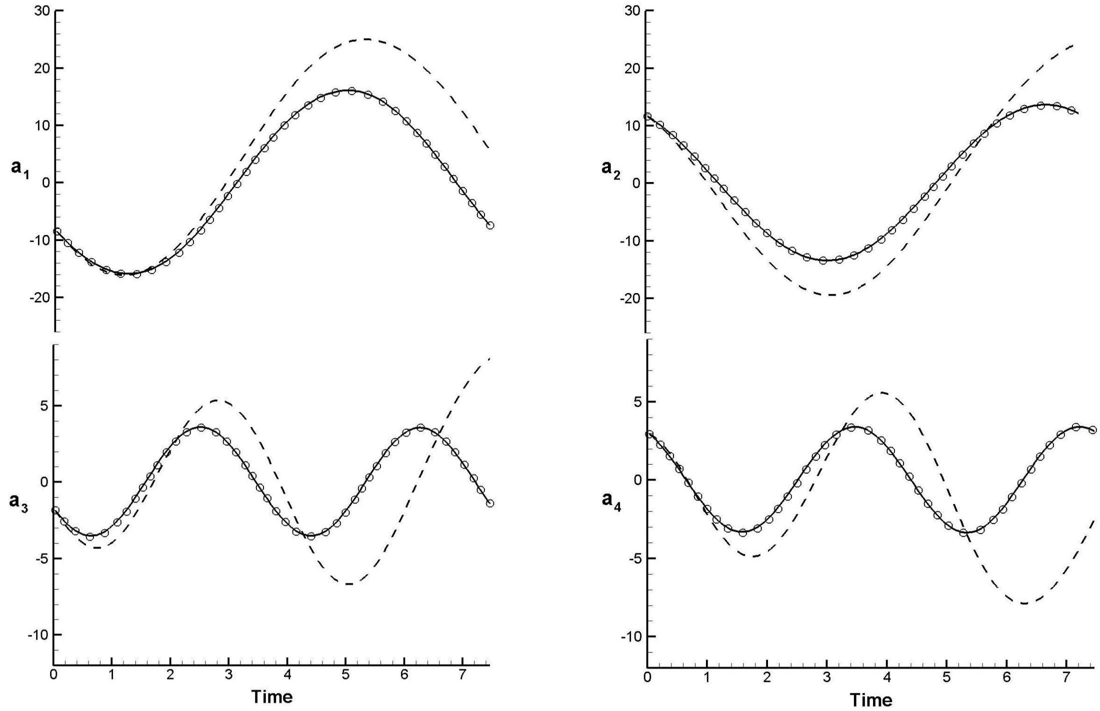

Fig. 3. Short time variations of the first four modal coefficients of streamwise velocity component at $R_e = 100$, (○ DNS), (– – – Classical POD reduced order model) and (— Calibrated POD reduced order model).

Fig. 4 shows the time variations of the first four modal coefficients of transverse velocity component for classical and calibrated low-order models (compared to DNS data). It is clear from this figure that the calibrated model has relatively good agreements compared to the DNS data.

In Table 1, a comparison between the computational times of POD ROM and Direct Numerical Simulation in short time period has been presented. It is clear that the calibrated reduced order model is working much faster than the DNS solver.

Table1. Comparison between CPU times of short time modeling using calibrated POD reduced order model and direct numerical simulation

	time (second)
Direct Numerical Simulation	900
POD Basis function computations	60
Computations of reduced order model coefficients	30
Solution of calibrated reduced order POD model	20

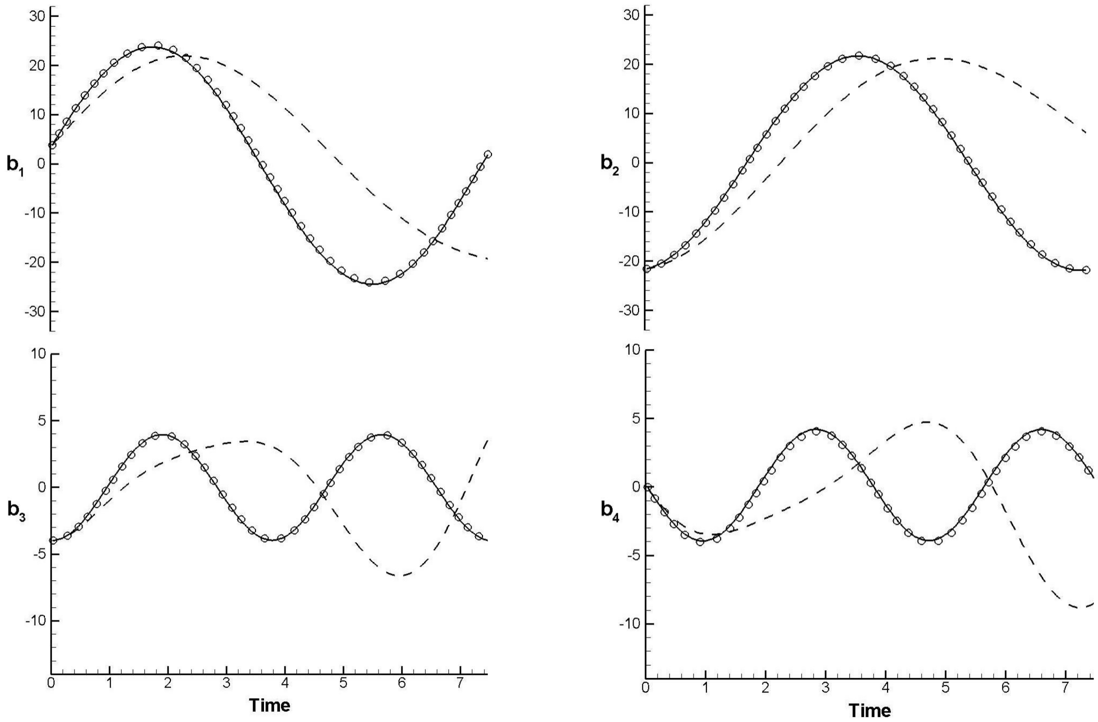

Fig. 4. Short time variations of the first four modal coefficients of transverse velocity component at $\mathrm{R_e}=100$, (○ DNS), (– – – Classical POD reduced order model) and (— Calibrated POD reduced order model).

In fig. 5, the reconstructed field of streamwise velocity component using DNS and the calibrated low-order POD model and the error between the DNS and the POD-ROM data are shown. It is obvious from this figure that the calibrated model predicts relatively accurate results and the related error in the entire field is very small.

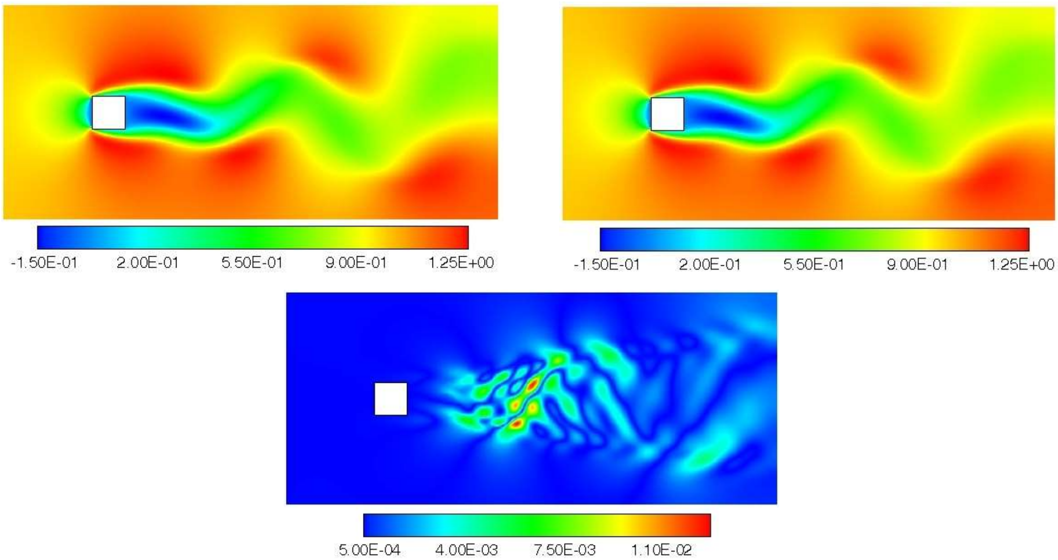

Fig. 5. Reconstructed streamwise velocity component field of a time step snapshot at $\mathrm{R_e}=100$, and related error between DNS and ROM data, DNS (Left-Top), calibrated POD-ROM model(Right-Top) and error between DNS and ROM(Bottom)

6.2 Linear Stability Analysis of Reduced Order Dynamical System

As noted before, there are systems whose trajectories separate exponentially in time. Indeed, there appears to be a dichotomy between systems for which nearby orbits separate linearly and “truly chaotic” systems whose orbits separate exponentially. For stability analysis of ODE systems, an eigenvalues analysis is usually used. Therefore, the Jacobian of the system is used for studying the sensitivity of the model. To compute the maximal Lyapunov exponent of a system of ODE's, both the original and the calibrated system must be integrated. The error in the computation is estimated by plotting the maximal Lyapunov exponent as a function of time. If the reduced order dynamical system is:

$$\frac{d\mathbf{a}^k}{dt}=f\,(\mathbf{a}), \tag{18}$$

The right hand side of Eq. (18) for the standard reduced order model is as:

$$f(\mathbf{a}) = -(\mathbf{A}_{kij}\mathbf{a}^i\mathbf{a}^j + \mathbf{B}_{ki}\,\mathbf{a}^i + \mathbf{C}_k), \tag{19}$$

For the calibrated reduced order model using combined POD and Fourier modes, it will as:

$$f(\mathbf{a}) = -\left(\mathbf{A}_{kij}\widehat{\mathbf{a}}^i\widehat{\mathbf{a}}^j + \left(\mathbf{B}_{ki} + \frac{\tilde{a}_o^{ki}}{2} + \sum_{n=1}^{N_f}\left[\tilde{a}_n^{ki}\cos\left(\frac{n\pi t}{T}\right) + \tilde{b}_n^{ki}\sin\left(\frac{n\pi t}{T}\right)\right]\right)\widehat{\mathbf{a}}^i + \mathbf{C}_k\right), \tag{20}$$

After linearization of dynamical system, the Jacobian of the reduced order dynamical system will be:

$$D = \frac{\partial}{\partial \mathbf{a}^k}(f(\mathbf{a})) \tag{21}$$

Therefore, the Jacobians of the calibrated and the standard ROM are:

$$D(\mathbf{a}) = -\left(\mathbf{A}_{kij}\mathbf{a}^i + \mathbf{B}_{ki}\right) \tag{22}$$

$$D(\mathbf{a}) = -\left(\mathbf{A}_{kij}\widehat{\mathbf{a}}^i + \left(\mathbf{B}_{ki} + \frac{\tilde{a}_o^{ki}}{2} + \sum_{n=1}^{N_f}\left[\tilde{a}_n^{ki}\cos\left(\frac{n\pi t}{T}\right) + \tilde{b}_n^{ki}\sin\left(\frac{n\pi t}{T}\right)\right]\right)\right), \tag{23}$$

Fig. 6 shows the time variations of maximum Lyapunov exponent for both velocity components in short time periods. Close agreements between eigenvalues of the calibrated reduced order model and the direct numerical simulation is observed in these figures, while the classical model deviates right after the beginning. It is clear that the calibrated low order model is adequately stable.

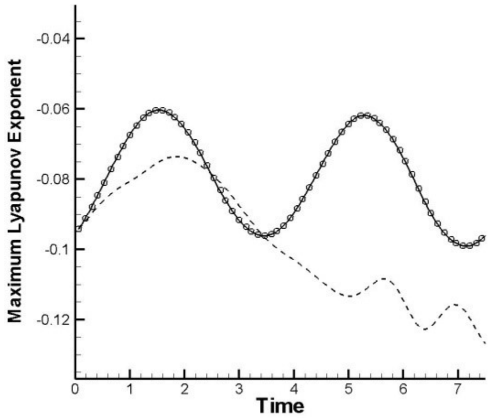

Fig. 6. Distribution of maximum Lyapunov exponent versus time for streamwise (left) and transverse (right) velocity components (○ DNS), (– – – Classical POD reduced order model) and (— Calibrated POD reduced order model).

An equilibrium point of a differential equation is stable if all the eigenvalues of the Jacobian matrix evaluated at this point have negative real parts. The equilibrium point is unstable if at least one of the eigenvalues has a positive real part. Fig. 7 shows the phase diagram of the Jacobian matrix eigenvalues of linearized calibrated reduced order dynamical system. These matrices are generated for both velocity components in short time period. In these figures, the real parts of the eigenvalues are negative in both reduced order dynamical systems. The more negative real part values demonstrate that the outcome ROMs are more stable than the related standard ROMs.

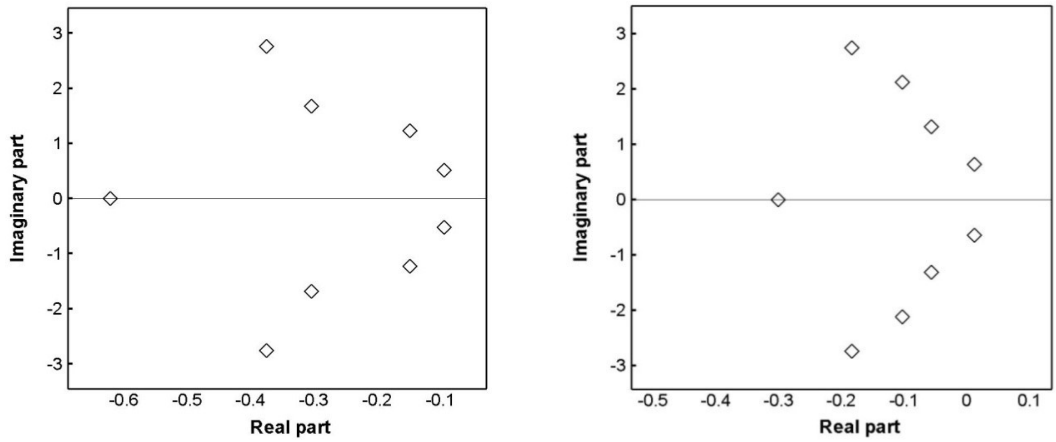

Fig. 7. Phase diagram of Jacobian matrix eigenvalues of the linearized dynamical system of velocity components, calibrated ROM of streamwise velocity (left) and transverse velocity components (right).

6.3 Long Time Period Simulation

In this section, the results obtained from both the classical and the calibrated reduced order models in long time periods are presented. Our test case has a periodic behavior in time and a stable manifold. The stable manifold of periodic orbit is the set of points such that the forward orbit starting from a point approaches the closed curve traced out by periodic orbit. Therefore, the obtained low-order model behaves as a periodic orbit dynamical system. It was mentioned in Section 4.2 that applying Fourier modes extension to reduced order model will lead to an autonomous dynamical system. Therefore, the classical and the calibrated low-order models are integrated in long time for four periods.

Fig. 8 shows the time variations of the first six modal coefficients of the streamwise velocity component obtained from the classical POD model. This figure affirms that the model deviates right at the beginning from the DNS data and has an unstable manifold. The unstable manifold for periodic orbit is the set of points such that the orbit going backward in time approaches the closed curve traced out by the periodic.

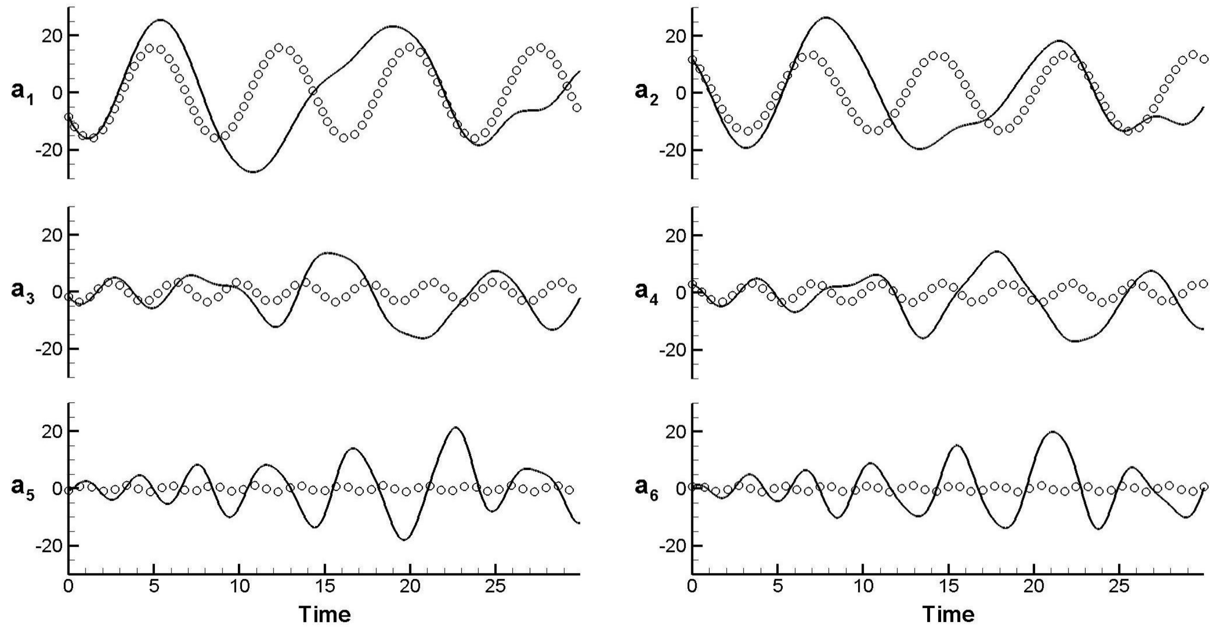

Fig. 8. Long time variations of the first six modal coefficients of streamwise velocity component at $R_e = 100$, (○ DNS) and (— Classical POD reduced order model).

Fig. 9 displays the time variations of the first four modal coefficients of the streamwise velocity component. These results were computed using the reduced order POD model with the pressure term representation. It is clear from this figure that the results are relatively erroneous. Therefore, the surrogate dynamical system diverges slowly from the snapshots projected data into the POD modal space.

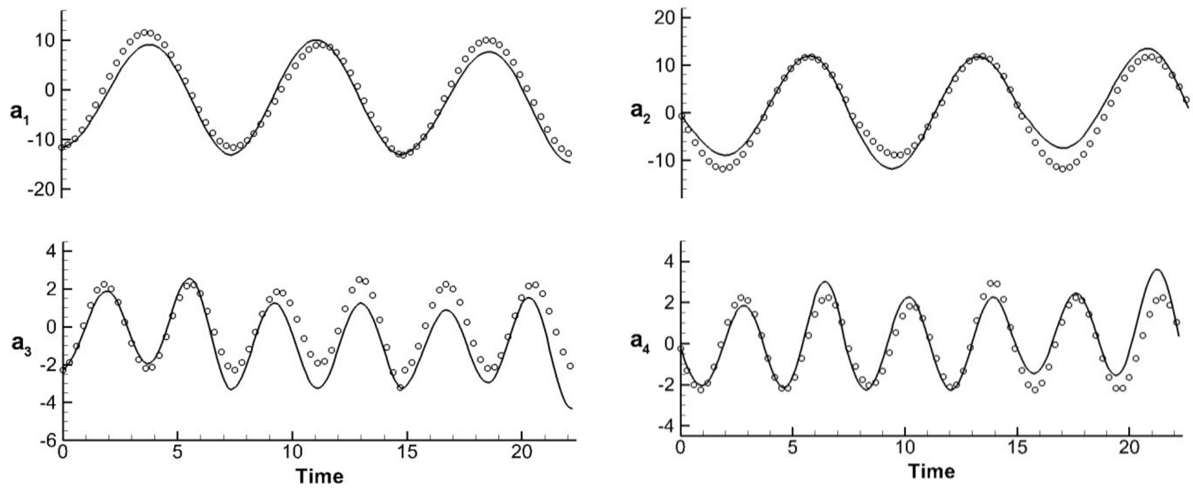

Fig. 9. Long time variations of the first four modal coefficients of streamwise velocity component at $R_e = 100$, (○ DNS) and (— POD reduced order model with pressure term correction).

Fig. 10 illustrates the variations of the first six modal coefficients of the streamwise velocity component as a function of time. These coefficients were obtained from the calibrated reduced order model and show that the model performs accurately enough in long time periods.

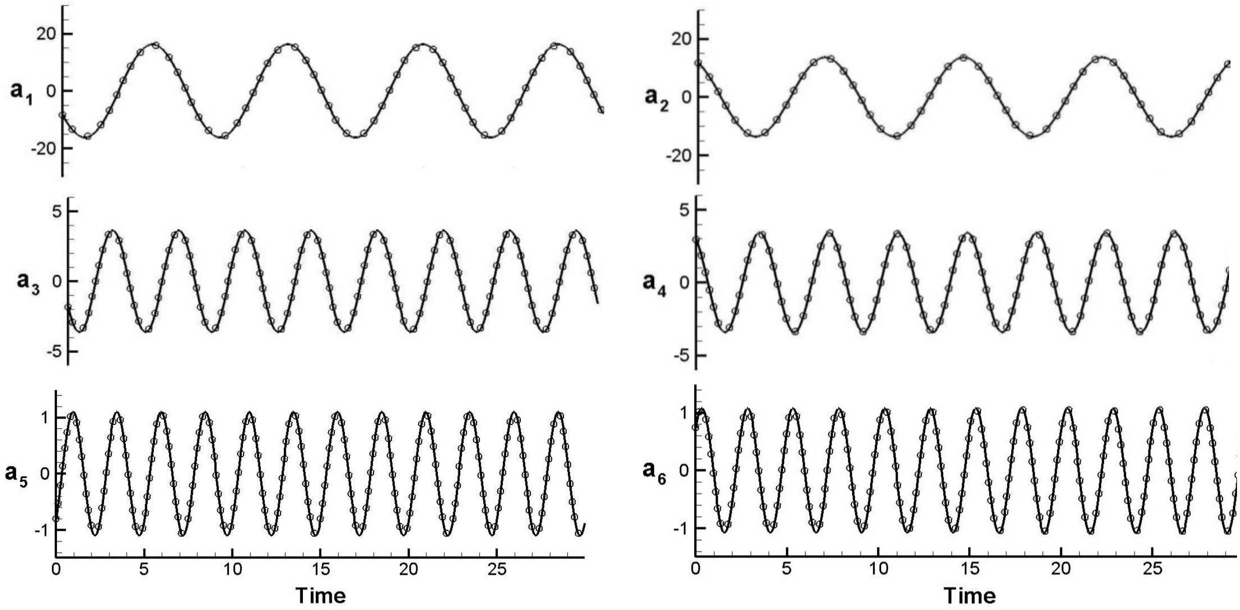

Fig. 10. Long time variations of the first six modal coefficients of streamwise velocity component at $R_e=100$, (○ DNS) and (— Calibrated POD reduced order model).

In Fig.11, the time variations of the first six modal coefficients of transverse velocity component, which were computed using the classical reduced order POD model, are shown. It is clear from this figure that the results are erroneous and similar to the streamwise velocity component. The related dynamical system diverges exponentially from the snapshots projection data.

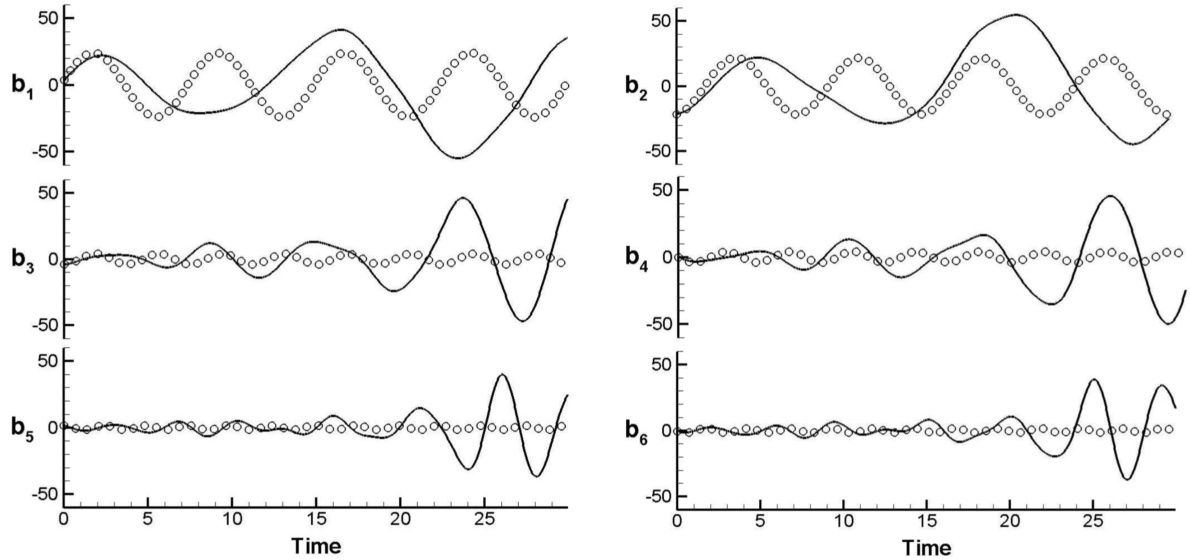

Fig. 11. Long time variations of the first six modal coefficients of transverse velocity component at $R_e=100$, (○ DNS) and (— Classical POD reduced order model).

Fig. 12 shows time variations of the first four modal coefficients of the streamwise velocity component, which were computed using the reduced order POD model with pressure term correction. It is obvious that the outcome results are relatively incorrect. Accordingly, the reduced order model predicted results contain slight deviations from DNS projected data into POD modal space. Fig. 13 shows the variations of the first six modal coefficients of transverse velocity component versus time. It is obvious from this figure that the simulations using the calibrated reduced order model are adequately accurate and the obtained model has close agreements to the DNS data in long time periods. In Table 2, the computational times of POD ROM and DNS solver in long time periods have been compared. It is obvious that the calibrated reduced order model is working much faster than the DNS solver.

Table2: Comparison between CPU time of long time modeling using calibrated POD reduced order model and direct numerical simulation (4 cycles)

	time (second)
Direct Numerical Simulation	3600
POD Basis function Computations	60

Computations of Reduced Order Model Coefficients	30
Solution of Calibrated Reduced Order POD Model in Short time period	20
Computations of Calibration term Coefficients using Fourier Modes	30
Solution of Calibrated Reduced Order POD Model in Long time period	80

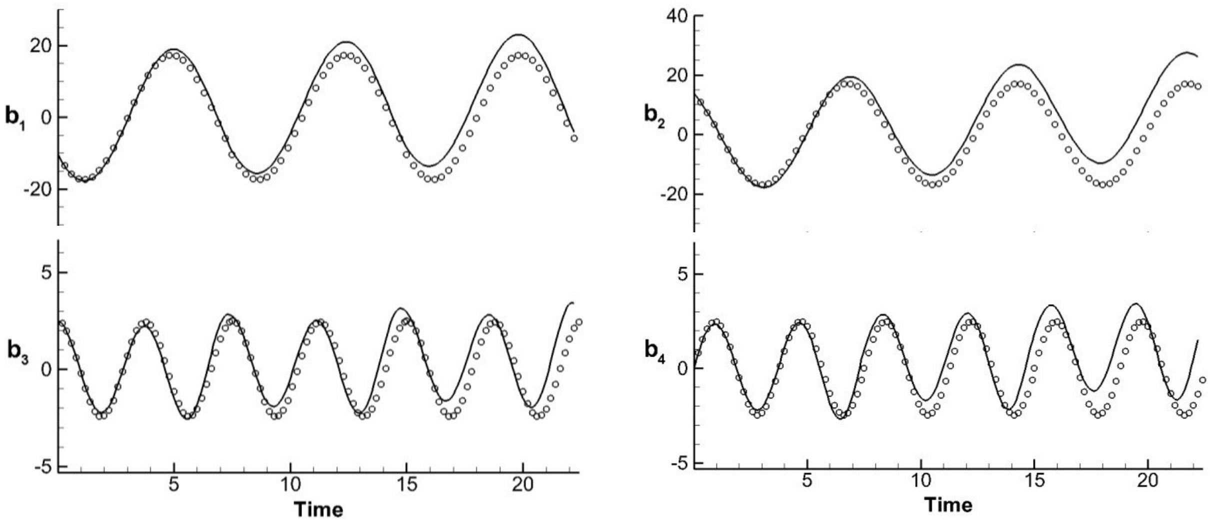

Fig. 12. Long time variations of the first four modal coefficients of transverse velocity component at $R_e=100$, (○ DNS) and (—POD reduced order model with pressure term correction).

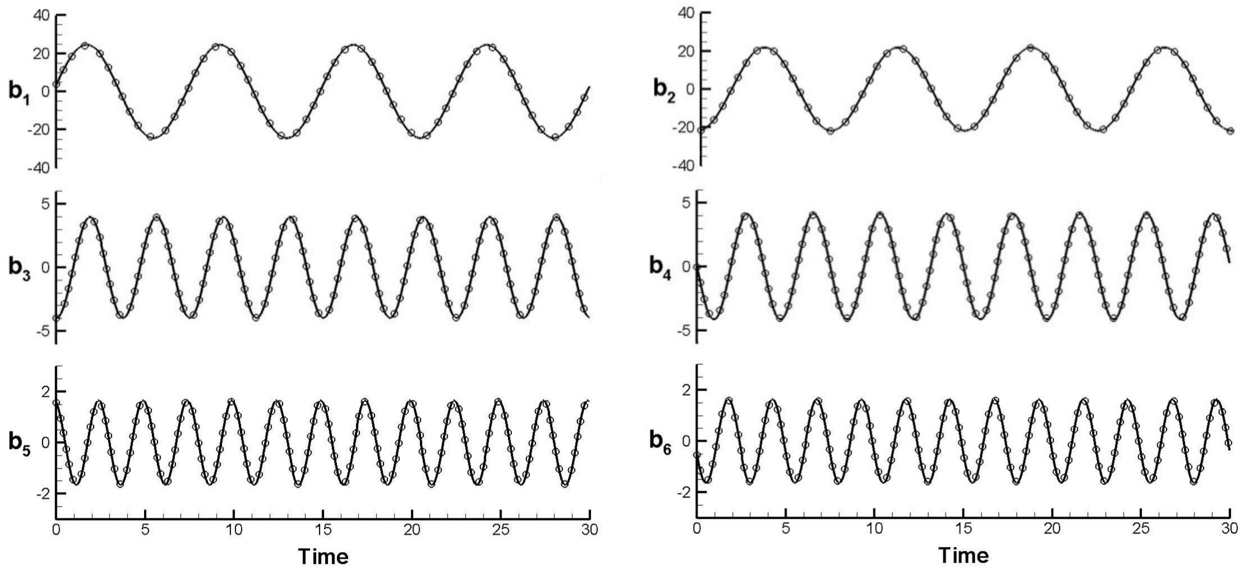

Fig. 13. Long time variations of the first six modal coefficients of transverse velocity component at $R_e=100$, (○ DNS) and (— Calibrated POD reduced order model).

7. Conclusions

In recent years, a significant progress has been made in advancing the state-of-the-art proper orthogonal decomposition (POD)-based reduced-order modeling (ROM). The improvement of this method for more accurate prediction of the flow field is often discussed in the literature. To this effect, this paper contributes to a new extension of dynamical system calibration for POD-based ROM methodology and demonstrates its suitability for the unsteady incompressible flow past a square cylinder. It is clear that the POD is a robust method for the estimation and simulation of the steady and unsteady flows, respectively. In this work, a POD snapshots method was used to calculate the POD modes. By projection of the Navier-Stokes equations along the POD modes, the reduced order dynamical system was reconstructed as an initial value problem. For damping the effects of the high level energy modes or repairing some effects of our assumptions in the reconstruction of the model, a local minimization scheme was used, which calibrated the dynamical system. An order-reduction manner was used to choose the minimum number of modes for reconstructing the dynamical system. Therefore, it prepares a Reduced Order model for the fast prediction of the flow field. Moreover, using the order reduction manner based on the calibration strategy, a smaller number of modes can be used for the reconstruction of the dynamical system. However, it does not perform accurately every time. The present method is used for wide range of time advancement and for both short and long time integrations. The current dynamical system gives suitable results. In other words, the present dynamical system is stable and performs accurately.

Conflict of Interest

The authors declare no conflict of interest.

References

[1] Couplet, M., Basdevant, C., Sagaut, P., Calibrated Reduced-order POD-Galerkin System for Fluid Flow Modeling, *J. Comp. Physics* 207, 2005, 192–220.
[2] Favier, J., Cordier, L., Kourta, A., Iollo, A., Calibrated POD Reduced-order Models of Massively Separated Flows in the Perspective of Their Control, ASME Joint U.S.-European Fluids Eng. Summer Meeting, Miami, Florida, USA, 2006.
[3] Galletti, B., Bruneau C.H., Zannetti L., Iollo, A., Low-order Modeling of Two-dimensional Flow Regimes Past a Confined Squared Cylinder, *J. Fluid Mech.* 503, 2004, 161-170.
[4] Holmes, P., Lumley, J.L., Berkooz, G., Turbulence, Coherent Structures, Dynamical Systems and Symmetry, Cambridge Monographs on Mechanics, Cambridge University Press, 1996.
[5] Li, H., Luo, Z., Gao, J., A New Reduced-Order FVE Algorithm Based on POD Method for Viscoelastic Equations, *Acta Mathematica Scientia*, Vol. 33, Issue 4, 2013, 1076-1098.
[6] Chen, J., Han, D., Yu, B., Sun, B., Wei, J., POD-Galerkin reduced-order model for viscoelastic turbulent channel flow, *Numerical Heat Transfer, Part B: Fundamentals*, 72(3), 2017, 268-283.
[7] Moayyedi, M.K., Low-dimensional POD simulation of Unsteady Flow around Bodies with Arbitrary Shapes, PhD Dissertation, Sharif University of Technology, 2009.
[8] Moayyedi, M.K., Taeibi-Rahni, M., Sabetghadam, F., Accurate Low-dimensional Dynamical Model for Simulation of Unsteady Incompressible Flows, The 12th Fluid Dynamics Conference, Babol, Iran, 2009.
[9] Noack, B.R., Papas, P., Monkewitz, P.A., The Need for a Pressure-term Representation in Empirical Galerkin Models of Incompressible Shear Flows, *J. Fluid Mech.* 523, 2005, 339-365.
[10] Rowely, C.W., Model Reduction for Fluids, Using Balanced Proper Orthogonal Decomposition, *Int. J. Bifurcation & Chaos* 89, 2005, 110-119.
[11] Sabetghadam, F., Jafarpour, A., Ghaffari, S.A., α Regularization of the POD-Galerkin Dynamical System of the Kuramoto-Sivashinsky Equation, *Applied Mathematics and Computation* 218 (10), 2012, 6012-6026.
[12] Sabetghadam, F., Moayyedi, M.K., and Taeibi-Rahni, M., A Fast Approach for Temporal Calibration of Low-dimensional Dynamical Model for Simulation of Unsteady Incompressible Flows, The 9th Annual Conference of Iranian Aerospace Society, Science & Research Branch IAU, Tehran, Iran, 2010.
[13] Sirisup, S., Karnidakis, G.E., A Spectral Viscosity Method for Correcting the Long Term Behavior of POD Models, *J. Comp. Physics* 194, 2004, 92-116.
[14] Luo, Z., Li, H., Sun, P., Gao, J., A Reduced-order Finite Difference Extrapolation Algorithm based on POD Technique for the non-stationary Navier–Stokes Equations, *Applied Mathematical Modelling*, 37(7), 2013, 5464-5473.
[15] Luo, Z., Proper Orthogonal Decomposition-based Reduced-order Stabilized Mixed Finite Volume Element Extrapolating Model for the Non-stationary Incompressible Boussinesq equations, *J. Mathematical Analysis and Applications*, 425(1), 2015, 259-280.
[16] Moayyedi, M.K., Calibration of Reduced Order POD Model of Unsteady Incompressible Laminar Flow Using Pressure Representation as a Function of Velocity Field Modes, *Tabriz University Journal of Mechanical Engineering*, 48(2), 2018, 349-358.